Anomalous dispersion of the elastic constants at the phase transformation of the $PbMg_{1/3}Nb_{2/3}O_3$ relaxor ferroelectric

S. G. Lushnikov,[1] A. I. Fedoseev,[1] S. N. Gvasaliya,[2,*] and Seiji Kojima[3]
[1]*Ioffe Physical Technical Institute, 26 Politekhnicheskaya, 194021 St. Petersburg, Russia*
[2]*Laboratory for Neutron Scattering, ETHZ and Paul-Scherrer Institut, CH-5232 Villigen PSI, Switzerland*
[3]*Institute of Materials Science, University of Tsukuba, Tsukuba, Ibaraki 305-8573, Japan*
(Received 25 September 2007; revised manuscript received 26 January 2008; published 31 March 2008)

Results of the Brillouin light scattering studies of elastic properties of a relaxor ferroelectric lead magnesium niobate, $PbMg_{1/3}Nb_{2/3}O_3$, crystals in the temperature range from 870 to 30 K are presented. By using the experimental results, temperature dependences of elastic C_{11}, C_{12}, and C_{44} constants have been built. Analysis of the temperature dependences of elastic constants has revealed anomalies in the vicinity of the Burns temperature ($T_B \approx 620$ K) and a suppressed ferroelectric phase transition ($T_c \approx 210$ K) that occurs when an external electric field is applied. A comparative analysis of the behaviors of elastic constants at different probe frequencies derived from our Brillouin scattering results and ultrasonic [G. A. Smolenskii *et al.*, Sov. Phys. Solid State **27**, 801 (1985)] measurements has been carried out. The remarkable dispersion in the relative variations of elastic C_{11} and C_{44} constants with decreasing temperature below the transition temperature into a cubic anisotropic phase ($T_M \approx 370$ K) has been found. These anomalous elastic behaviors related to three typical transition temperatures are discussed as the peculiar natures of relaxor ferroelectrics.

DOI: 10.1103/PhysRevB.77.104122 PACS number(s): 62.65.+k, 77.84.Dy, 77.84.−s, 78.35.+c

Relaxor ferroelectrics belonging to the family of complex perovskites are promising materials for piezoelectric and electro-optic devices, condensers, etc.[1] From the point of view of basic research, cubic relaxor ferroelectrics are model objects for investigations of the effect of disordering on the lattice dynamics. Indeed, the introduction of B' and B'' ions with different valencies into a B sublattice of a perovskite ABO_3 structure gives rise to a diffuse frequency-dependent maximum in the dielectric response and broad anomalies in the temperature behavior and many unique physical characteristics of relaxors.[2] However, in spite of the fact that relaxor ferroelectrics have been intensively studied by dielectric,[3] optical,[4] neutron[5] spectroscopy, and other techniques,[6] no complete self-consistent picture of the crystalline lattice dynamics in these compounds has been obtained so far.

A lead magnesium niobate crystal [$PbMg_{1/3}Nb_{2/3}O_3$(PMN)] is a typical representative of relaxor ferroelectrics which were synthesized in the 1950s. Now, this material is among the most thoroughly studied compounds of the family of complex perovskites with the common formula $AB'B''O_3$. A characteristic feature of PMN is the absence of a structural phase transition down to 5 K.[7] A ferroelectric phase transition can be induced in the vicinity of $T_c = 210$ K under an applied electric field that exceeds a threshold value.[8] The dielectric response demonstrates a frequency-dependent anomaly spreading for several hundreds of degrees with a maximum in the vicinity of 270 K at 10 kHz.[3] The anomalous behavior of many physical properties of PMN is believed to be due to polar nanoregions (PNRs) that appear in the vicinity of the Burns temperature ($T_B \approx 620$ K).[9] The elastic properties of PMN have been extensively studied by the Brillouin light scattering[10–16] and ultrasonic techniques.[17,18] Wide minima in the temperature dependences of C_{11} and C_{44} elastic constants and a maximum in that of C_{12} in the vicinity of 270 K were revealed. It was found later that these anomalies are frequency dependent and shift toward higher temperatures with increasing measuring frequencies,[11,12] but the attempts to invoke fluctuation mechanisms or relaxation time distribution to explain these anomalies were not successful.[12] In recent inelastic neutron scattering investigations of the low-frequency vibrational spectra of PMN, 0.68PMN-0.32PT, and related crystals of PMT, the quasielastic scattering originated from a relaxation mode was found.[19,20] It is observed that the damping of the phonons increases in the temperature range where the susceptibility of the quasielastic scattering associated with the relaxation mode is significant. These findings necessitate further studies of the behavior of acoustic phonons in PMN. The present paper describes the results obtained in the experimental investigations of elastic properties of PMN crystals by the Brillouin light scattering and presents a comparative analysis of these results with literature data. Such an approach can give an insight into the behavior of elastic constants of PMN at frequencies ranging from 30 MHz to 50 GHz.

In the Brillouin light scattering experiments, a 3+3-pass Fabry–Perot interferometer (J. Sandercock tandem) equipped with an optical microscope was used. A source of scattered light excitation was an Ar^+ ion laser with a wavelength $\lambda_0 = 514.5$ nm. The radiation power did not exceed 100 mW. In this case, a 180° experimental geometry was used, and the samples were mounted in a cell (THMS 6000) where temperature was smoothly decreased from 870 to 80 K, with a stabilization of ±0.1 K. The 90° experimental geometry involved the use of a home-made furnace and an optical cryostat where temperature variations were controlled with a digital temperature controller (SI9650/Lakeshore331) and closed-cycle helium refrigerator (RMC LTS-22), respectively.

Measurements were carried out on three types of sample in two scattering geometries (examples of experimental spec-

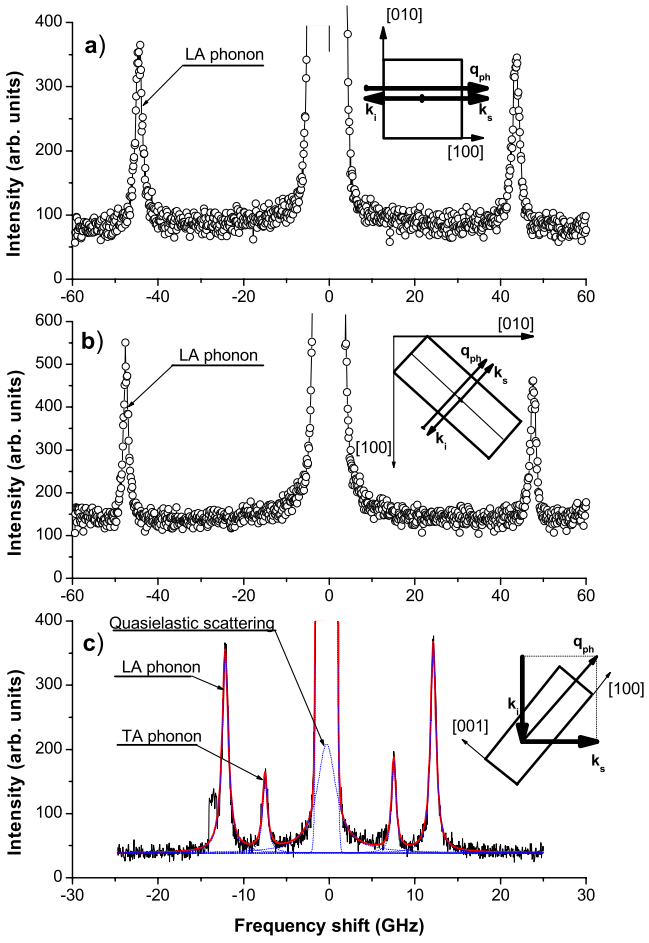

FIG. 1. (Color online) Experimental spectrum of the Brillouin light scattering at room temperature in the [(a) and (b)] 180° scattering geometry and (c) 90 A geometry of scattering.

tra are shown in Fig. 1). The PMN samples in the form of parallelepipeds of $\sim 7\times 5\times 5$ mm^3 in size with the facets oriented along the [001], [010], and [001] directions were studied in the 180° geometry of scattering. In this geometry [see the inset of Fig. 1(a)], light scattering from acoustic phonons with wave vector $\mathbf{q}_{\rm ph}\|[001]$ was investigated. The incident and scattered light were polarized along [010]. According to selection rules,[21] the light scattering spectra in this case have one longitudinal acoustic (LA) phonon whose frequency shift $\Delta\nu_{11}^a$ is given by

$$V_{11}^a = \frac{\lambda_0 \Delta \nu_{11}^a}{2n}, \quad \rho (V_{11}^a)^2 = C_{11}^a, \tag{1}$$

where V_{11}^a is the sound velocity, and n, ρ, and C_{11}^a are the refractive index, density, and elastic constant of the crystal studied, respectively. The a index (and also the b and c indices in the subsequent discussion) denotes the experimental geometry.

The samples in the form of rectangular PMN plates cut perpendicularly to the $[1\bar{1}1]$, [110], and [001] directions were studied in the 180° geometry of scattering. In this geometry, a temperature behavior of a LA phonon with $\mathbf{q}_{\rm ph}\|[110]$ was investigated. The incident and scattered light were polarized along [001] [geometry b, see the inset of Fig. 1(b)]. The frequency shift $\Delta\nu^b$ of this phonon was defined, according to Ref. 21, as

$$V^b = \frac{\lambda_0 \Delta \nu^b}{2n}, \quad \rho (V^b)^2 = C^b = \tfrac{1}{2}(C_{11}^b + C_{12}^b) + C_{44}^b. \tag{2}$$

For the experiments in the 90 A scattering geometry [geometry c, Fig. 1(c)], samples in the form of ~1-mm-thick plane-parallel plates with the plane normal to the [001] direction were used. In this geometry, scattering from acoustic phonons with $\mathbf{q}_{\rm ph}\|[100]$ was examined [Fig. 1(c)]. The incident and scattered light were polarized along [010]. In this geometry, the light scattering spectra of a PMN crystal exhibit a longitudinal (LA) and transverse (TA) phonons. The frequency shifts of these modes, $\Delta\nu_{11}^c$ and $\Delta\nu_{44}^c$, are defined by expressions (3) and (4), which do not include a refractive index,[22]

$$V_{11}^c = \frac{\lambda_0 \Delta \nu_{11}^c}{\sqrt{2}}, \quad \rho (V_{11}^c)^2 = C_{11}^c, \tag{3}$$

$$V_{44}^c = \frac{\lambda_0 \Delta \nu_{44}^c}{\sqrt{2}}, \quad \rho (V_{44}^c)^2 = C_{44}^c, \tag{4}$$

where V_{11}^c and V_{44}^c are the velocities of the longitudinal and transverse phonons, respectively, and C_{11}^c and C_{44}^c are the corresponding elastic constants.

A free spectral interval of the Fabry–Perot tandem interferometer was 30 GHz or 75 GHz, depending on the experimental geometry. The experimental room-temperature spectra whose examples are shown in Fig. 1 were processed by the least squares method. The fitting functions in calculations of phonon line shapes and scattering at an unshifted frequency were the Lorentz and Gauss functions, respectively. It is well seen from Fig. 1(c) that there is an additional contribution at the unshifted frequency, i.e., the quasielastic scattering described by the Lorentz function. (The behavior of the quasielastic scattering with varying temperature will be discussed elsewhere.)

By using the obtained frequency shifts, the mass density ρ=8.12 g/cm^3,[23] and the temperature dependence of the refractive index for PMN taken from Ref. 9, we calculated temperature dependences of C_{11}^a at the frequency of measurements $f\sim 45.5$ GHz, C_{11}^c at $f\sim 12.5$ GHz, C_{44}^c at $f\sim 8$ GHz, $C^b=0.5(C_{11}^b+C_{12}^b)+C_{44}^b$ at $f\sim 48.5$ GHz (see Fig. 2, curves 1–3, respectively), and C_{44}^c at $f\sim 8$ GHz (see Fig. 3, curve 1). The elastic constants of the PMN crystal at room temperature (see Table I and their temperature behaviors were found to be consistent with the literature data.[16,17] However, it should be noted that the magnitude of C_{11} depends on the probe frequency (and consequently on the wave vector) (see Fig. 2 and Table I). It can be seen from Fig. 2 that C_{11} monotonically grows with increasing frequency in the temperature range of 800–200 K. A more complicated picture is observed in the temperature region below 200 K: C_{11} exhibits frequency dependence at ~45 and ~12 GHz and does not vary with frequency between 12 GHz and 30 MHz. For the C_{44} elastic constant, the differences between the ultrasonic and the Brillouin measurements are observed in the tempera-

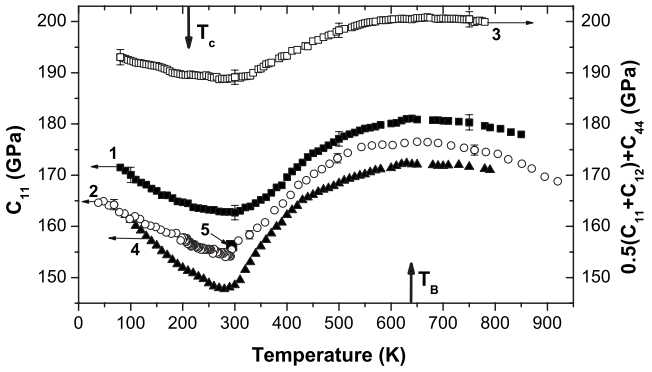

FIG. 2. Temperature dependences of the C_{11} (curves 1 and 2) and of the $C^b(T)=0.5[C^b_{11}(T)+C^b_{12}(T)]+C^b_{44}(T)$ (curve 3) elastic constants obtained at different scattering geometries in the Brillouin experiments (see text in detail). Curve 4 shows the temperature behavior of the C_{11} elastic constant taken from ultrasonic measurements at the frequency $f=30$ MHz. (Ref. 17). A solid square 5 is taken at room temperature by the Brillouin light scattering (Ref. 16).

ture regions from 750 to 400 K and below 200 K (Fig. 3). Unlike the case of the C_{11} elastic constant, outside the range of the dielectric anomaly, the higher values of the C_{44} elastic modulus are observed at the lower frequency.

Figure 4 (curve 1) shows the temperature dependence of C_{12} for PMN calculated from $C^a_{11}(T)$, $C^c_{44}(T)$, and $C^b(T)=0.5[C^b_{11}(T)+C^b_{12}(T)]+C^b_{44}(T)$ under the condition that the dispersions of elastic moduli are neglected, or, in other words, it is assumed that $C^a_{11}\equiv C^b_{11}(T)$ and $C^b_{44}\equiv C^c_{44}$.

Analysis of the temperature dependences of C_{ij} obtained in our investigations has revealed two characteristic anomalies in the vicinity of $T_B\sim 620$ K and $T_c\sim 210$ K (Figs. 2–4). Let us consider the behaviors of C_{11} and C_{44}. It can be seen from Fig. 2 that the temperature dependence of C_{11} exhibits, in addition to a broad minimum at $T\approx 270$ K, weak anomalies in the form of "bends" in the vicinity of the Burns temperature, and T_c that manifest themselves at all frequencies

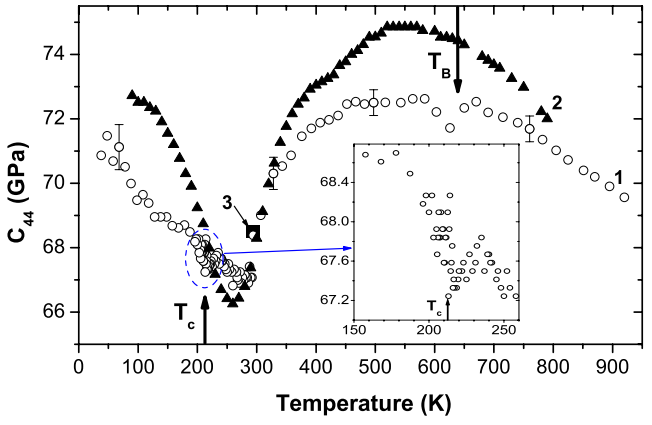

FIG. 3. (Color online) Temperature dependences of C_{44} elastic constants at hypersonic (curve 1) and ultrasonic (curve 2 from Ref. 17) frequencies. A solid square 3 is taken at room temperature by the Brillouin light scattering (Ref. 16).

and are most pronounced at 12 GHz. The anomaly in the temperature dependences of C_{11} in the vicinity of T_B is likely to be attributable to the formation of PNRs, and the anomaly at $T_c=210$ K can be due to a suppressed structural phase transition.

In the temperature dependence of C_{44} obtained in the Brillouin measurements, three characteristic portions can be separated out. At $T>T_B$, C_{44} decreases with increasing temperature, which is typically attributed to the crystalline lattice anharmonicity. In the region 380 K$<T<T_B$, the C_{44} is nearly temperature independent. Probably, this is due to a strong interaction between the transverse acoustic mode responsible for the behavior of the C_{44} elastic modulus and low-lying transverse optical mode discussed for the wave vectors away from the zone center in Ref. 19. Starting from $T<370$ K a 7% softening of C_{44} is observed; it has a minimum in the vicinity of 280 K, after which it begins to grow monotonically with decreasing temperature and experiences a weak anomaly in the vicinity of T_c (see the inset of Fig. 3). It can be seen from Fig. 4 that the temperature dependence of C_{12} also has anomalies in the vicinity of T_c and T_B.

As a whole, the behaviors of the C_{ij} in PMN are similar to expected behavior for the elastic constant in the vicinity of a phase transition if the strain is a secondary order parameter. However, a very unusual feature in case of PMN is that these anomalies are extended over much broader temperature range.

We consider now in more detail the behaviors of C_{11} and C_{44} at different probe frequencies. To this end, we plot the dependence of relative variations in these elastic constants $\delta C_{11}(T)=[C_{11}(T)-C_{11}(T_0)]/C_{11}(T_0)$ and $\delta C_{44}(T)=[C_{44}(T)-C_{44}(T_0)]/C_{44}(T_0)$. The zero points ($T_0$) are chosen to be the values of C_{11} and C_{44} at $T=690$ K (Fig. 5), where we assume that the acoustic phonons seem to show conventional behavior typical for a weakly anharmonic crystal. It is well seen from Fig. 5(a) that δC_{11} behaves in a similar manner at all frequencies above 370 K (within the measuring accuracy). A decrease of temperature below 370 K leads to differences in the behavior of $\delta C_{11}(T)$ at different frequencies. It is interesting to note that in the region of low temperatures (around 120 K), the behaviors of $\delta C_{11}(T)$ in the low- (30 MHz) and high-frequency (~45 GHz) limits again coincide. The intermediate dependence (at frequencies of the order of 12 GHz) exhibits a difference from the high-frequency data up to 50 K. Of interest is the fact that the temperature at which the dispersion in the behavior of $\delta C_{11}(T)$ arises coincides with the temperature at which a growth in the neutron elastic central peak intensity, a change in the behavior of inverse correlation length of the neutron quasielastic scattering, and a maximum in the dielectric susceptibility measured at frequency 10 GHz are observed.[19] In Ref. 19, such behaviors of the central peak, susceptibility, and correlation length were explained by a transition at $T_M=370$ K into a phase where the cubic anisotropy starts to play a role. It is likely that this transition manifests itself in the dynamic behavior of PMN elastic properties as well. The temperature dependencies of δC_{44} [Fig. 5(b)] become different at the Burns temperature, again coincide in the vicinity of 400 K, and at $T<370$ K, they again diverge. The dispersion is more pronounced with decreasing temperature below $T<370$ K and reaches a

TABLE I. Elastic constants for PMN crystal at room temperature.

Geometry of experiment	Probe frequency	C_{11}^E (GPa)	C_{44}^E (GPa)	C_{12}^E (GPa)	$0.5(C_{11}^E+C_{12}^E)+C_{44}^E$ (GPa)	Source
Ultrasound study	30 MHz	148.3	67.8	72.3		Ref. 17
32° geometry $\mathbf{q}_{ph}\|[100]$	~12.1 GHz ~8.1 GHz	149	67.6			Ref. 14
90 A geometry $\mathbf{q}_{ph}$ in (ab) plane	~11 GHz ~7 GHz	156.2 ± 3.4	68.5 ± 3.1	76.0 ± 3.9		Ref. 16
90 A geometry $\mathbf{q}_{ph}\|[100]$	~12.5 GHz ~8 GHz	155.3 ± 2.3	68.3 ± 2.1			This study
180° geometry $\mathbf{q}_{ph}\|[100]$	~45.5 GHz	162				Ref. 14
180° geometry $\mathbf{q}_{ph}\|[100]$ $\mathbf{q}_{ph}\|[100]$	~45.5 GHz ~48.5 GHz ~8 GHz	164.8 ± 2.0		78.4 ± 3.2	188.9 ± 2.0	This study

maximum in the vicinity of 260 K. Thus, the behavior of $\delta C_{44}(T)$ at $T<370$ K exhibits a considerable dispersion, similar to that observed for $\delta C_{11}(T)$. A plausible hypothesis of the origin of the dispersion effects is frequency-dependent anharmonic contribution to the elastic constants of PMN. The relative magnitude of the effect in PMN is comparable with the difference of the elastic constants of alkali halides taken in the region of the first and the zero sound at 300 K.[24] In order to quantitatively analyze possible mechanisms of dispersion of the elastic moduli in the PMN crystals, acoustic measurements should be carried out in a wide frequency range and more information on the phonon dispersion curves to be obtained.

To summarize, temperature dependences of all elastic constants of PMN crystals have been investigated. The results obtained suggest that the elastic subsystem of PMN crystals is sensitive to minor changes in the crystalline lattice dynamics: anomalies below the Burns temperature ($T_B \approx 620$ K) and in the vicinity of the suppressed structural phase transition ($T_c \approx 210$ K) and transition into a cubic

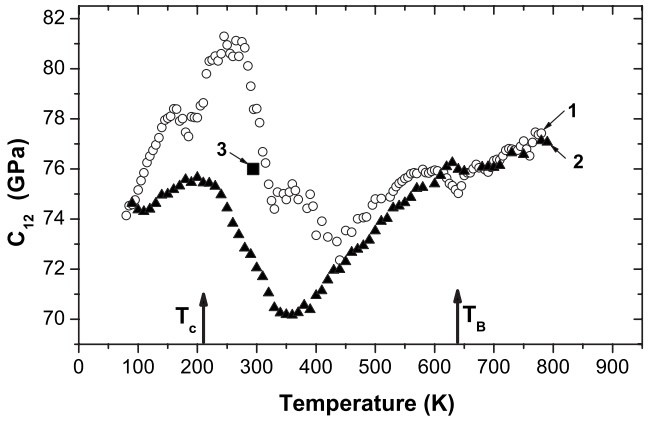

FIG. 4. Temperature dependences of C_{12} elastic constants at hypersonic (calculated curve 1, see text) and ultrasonic (curve 2 from Ref. 17) frequencies. A solid square 3 is taken at room temperature by the Brillouin light scattering (Ref. 16).

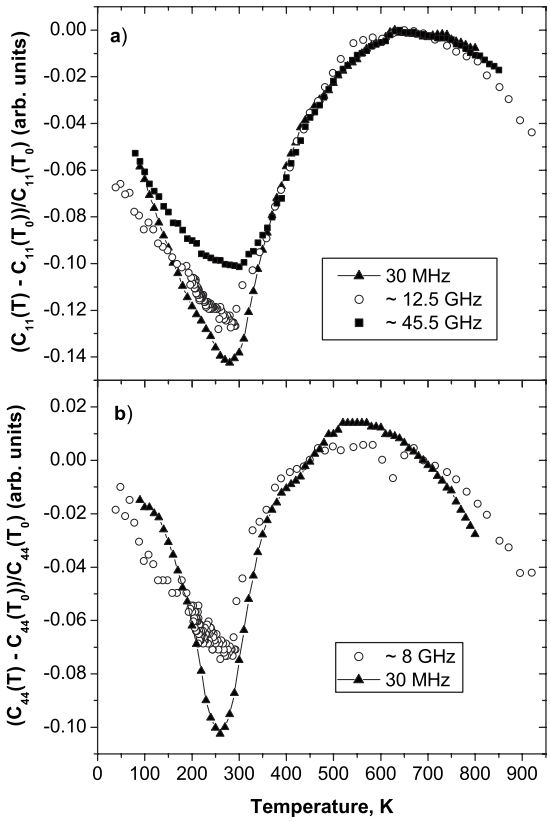

FIG. 5. Temperature evolution of relative changes in the elastic constants (a) C_{11} and (b) C_{44} has been obtained at different probing frequencies.

anisotropic phase ($T_M \approx 370$ K) are observed. The magnitudes and behaviors of elastic $\delta C_{11}(T)$ and $\delta C_{44}(T)$ constants were found to depend on the probe frequency.

The authors would like to thank R. A. Cowley for helpful discussions. This research was partially supported by the RFBR under Grant No. 05-02-17822 and by a grant from the President of the Russian Federation (SS-2168.2003.2). One of the authors (S.G.L.) is thankful to JSPS for support and to Institute of Materials Science, University of Tsukuba, for hospitality.

*On leave from Ioffe Physical Technical Institute, 26 Politekhnicheskaya, 194021 St. Petersburg, Russia.

[1] H. Fu and R. E. Cohen, Nature (London) **403**, 283 (2000).

[2] G. A. Smolenskii, V. A. Bokov, V. A. Isupov, N. N. Krainik, R. E. Pasynkov, and A. I. Sokolov, *Ferroelectrics and Related Materials* (Gordon and Breach, New York, 1984).

[3] E. V. Colla, E. Y. Koroleva, N. M. Okuneva, and S. B. Vakhrushev, J. Phys.: Condens. Matter **4**, 3671 (1992); A. E. Glazounov and A. K. Tagantsev, Phys. Rev. Lett. **85**, 2192 (2000); Eugene V. Colla, Lambert K. Chao, and M. B. Weissman, Phys. Rev. B **63**, 134107 (2001); R. Pirc, R. Blinc, and Z. Kutnjak, *ibid.* **65**, 214101 (2002).

[4] I. G. Siny, S. G. Lushnikov, R. S. Katiyar, and V. H. Schmidt, Ferroelectrics **226**, 191 (1999); J. Kreisel, B. Dkhil, P. Bouvier, and J. M. Kiat, Phys. Rev. B **65**, 172101 (2002); S. Kamba, E. Buixaderas, J. Petzelt, J. Fousek, J. Nosek, and P. Bridenbaugh, J. Appl. Phys. **93**, 933 (2003); S. G. Lushnikov, S. N. Gvasaliya, and R. Katiyar, Phys. Rev. B **70**, 172101 (2004); B. Mihailova, M. Bastjan, B. Shulz, M. Ruebhausen, and M. Gospodinov, Appl. Phys. Lett. **90**, 042907 (2007).

[5] S. B. Vakhrushev, B. E. Kvyatkovsky, A. A. Nabereznov, N. M. Okuneva, and B. P. Toperverg, Physica B **156&157**, 90 (1989); S. N. Gvasaliya, D. Strauch, B. Dorner, S. G. Lushnikov, and S. Vakhrushev, Ferroelectrics **282**, 21 (2003); S. N. Gvasaliya, S. G. Lushnikov, I. L. Sashin, and T. A. Shaplygina, J. Appl. Phys. **94**, 1130 (2003); C. Stock, D. Ellis, I. P. Swainson, G. Xu, H. Hiraka, Z. Zhong, H. Luo, X. Zhao, D. Viehland, R. J. Birgeneau, and G. Shirane, Phys. Rev. B **73**, 064107 (2006).

[6] R. Blinc, A. Gregorovič, B. Zalar, R. Pirc, V. V. Laguta, and M. D. Glinchuk, Phys. Rev. B **63**, 024104 (2000); Yosuke Moriya, Hitoshi Kawaji, Takeo Tojo, and Tooru Atake, Phys. Rev. Lett. **90**, 205901 (2003); Jorge Íñiguez and L. Bellaiche, Phys. Rev. B **73**, 144109 (2006).

[7] N. de Mathan, E. Husson, G. Calvarin, J. R. Gavarri, A. R. Hewat, and A. Morell, J. Phys.: Condens. Matter **3**, 8159 (1991).

[8] G. Schmidt, H. Arndt, J. Voncieminski, T. Petzsche, H. Voigt, and N. N. Krainik, Krist. Tech. **15**, 1415 (1980).

[9] G. Burns and B. A. Scott, Solid State Commun. **13**, 423 (1973).

[10] G. A. Smolensky, S. D. Prokhorova, I. G. Siny, and E. O. Chernyschova, Izv. Akad. Nauk SSSR, Ser. Fiz. **41**, 611 (1977).

[11] R. Laiho, S. G. Lushnikov, S. D. Prokhorova, and I. G. Siny, Sov. Phys. Solid State **32**, 2024 (1990).

[12] R. Laiho, S. G. Lushnikov, and I. G. Siny, Ferroelectrics **125**, 493 (1992).

[13] I. G. Siny, S. G. Lushnikov, C.-S. Tu, and V. H. Schmidt, Ferroelectrics **170**, 197 (1995).

[14] C. S. Tu, V. H. Schmidt, and I. G. Siny, J. Appl. Phys. **78**, 5665 (1995).

[15] S. Lushnikov, J.-H. Ko, and S. Kojima, Appl. Phys. Lett. **84**, 4798 (2004); S. G. Lushnikov, A. I. Fedoseev, J.-H. Ko, and S. Kojima, Jpn. J. Appl. Phys., Part 1 **44**, 7156 (2005).

[16] M. Ahart, A. Asthagiri, Z.-G. Ye, P. Dera, H.-K. Mao, R. E. Cohen, and R. J. Hemley, Phys. Rev. B **75**, 144410 (2007).

[17] G. A. Smolenskii, N. K. Yushin, and S. I. Smirnov, Sov. Phys. Solid State **27**, 801 (1985).

[18] S. B. Dorogovtsev and N. K. Yushin, Ferroelectrics **112**, 27 (1990).

[19] S. N. Gvasaliya, S. G. Lushnikov, and B. Roessli, Phys. Rev. B **69**, 092105 (2004); S. N. Gvasaliya, B. Roessli, R. A. Cowley, P. Huber, and S. G. Lushnikov, J. Phys.: Condens. Matter **17**, 4343 (2005).

[20] S. N. Gvasaliya, B. Roessli, R. A. Cowley, S. Kojima, and S. G. Lushnikov, J. Phys.: Condens. Matter **19**, 016219 (2007).

[21] R. Vacher and L. Boyer, Phys. Rev. B **6**, 639 (1972).

[22] J. M. Vaughan, *The Fabry-Perot Interferometer* (Adam Hilger, Bristol, 1989).

[23] V. A. Bokov and I. E. Myl'nikova, Sov. Phys. Solid State **2**, 2428 (1961).

[24] R. A. Cowley, Proc. Phys. Soc. London **90**, 1127 (1967).